Ferrata Storti Foundation

Haematologica 2021
Volume 106(5):1278-1289

P2X7 promotes the progression of *MLL-AF9*-induced acute myeloid leukemia by upregulation of Pbx3

Wenli Feng,[#] Xiao Yang,[#] Lina Wang, Rong Wang, Feifei Yang, Hao Wang, Xiaoli Liu, Qian Ren, Yingchi Zhang, Xiaofan Zhu and Guoguang Zheng

State Key Laboratory of Experimental Hematology, National Clinical Research Center for Blood Diseases, Institute of Hematology & Blood Diseases Hospital, Chinese Academy of Medical Sciences & Peking Union Medical College, Tianjin, China

[#]WF and XY contributed equally as co-first authors.

ABSTRACT

Nucleotides mediate intercellular communication by activating purinergic receptors and take part in various physiological and pathological processes. Abnormal purinergic signaling plays important roles in malignant progression. P2X7, which belongs to the P2X family of purinergic receptors, is abnormally expressed in various types of malignancies including leukemia. However, its role and molecular mechanism of action in leukemia have not been elucidated. Here, we analyzed the correlation between P2X7 expression and clinical outcome in acute myeloid leukemia (AML); we explored the role and mechanism of P2X7 in AML progression by using mouse AML, nude mouse xenograft and patient-derived xenograft models. High levels of P2X7 expression were correlated with worse survival in AML. P2X7 was highly expressed in *MLL*-rearranged AML and accelerated the progression of this type of AML both by promoting cell proliferation and by increasing leukemia stem cells. Furthermore, P2X7 caused upregulation of Pbx3 which might account for its pro-leukemic effects. The P2X7-Pbx3 pathway might also contribute to the progression of other types of leukemia as well as solid tumors with high levels of P2X7 expression. Our study provides new insights into the progression of malignancy caused by abnormal purinergic signaling.

Correspondence:

GUOGUANG ZHENG
zhengggtjchn@aliyun.com

Received: November 19, 2019.

Accepted: March 6, 2020.

Pre-published: March 12, 2020.

https://doi.org/10.3324/haematol.2019.243360

Introduction

Aberrant cell signaling, caused by both genetic and epigenetic abnormalities, plays a vital role in the pathogenesis and development of malignancies.[1] Nucleotides, which have been suggested to be extracellular messengers for decades, play important roles under various physiological and pathological conditions by activating purinergic receptors.[2] P2X7, the latest cloned member of the P2X family of purinergic receptors, is abnormally expressed in solid tumors.[3] Calcium-triggered activation of the PI3K/AKT pathway and downstream ERK1/2 or P38 has been suggested to be involved in P2X7-dependent growth and invasiveness in solid tumors.[4,5] Subsequently, the increased release of tumor necrosis factor-α, vascular endothelial growth factor, matrix metalloproteinases or substance P was found to favor the proliferation, infiltration and metastasis of tumor cells. Abnormal expression of P2X7 was detected in patients with leukemia, especially those with relapsed acute leukemia and evolutive B-cell chronic lymphocytic leukemia (CLL).[6-8] Furthermore, a hyposensitive P2X7 mutant was cloned from leukemia cells.[9,10] These results imply that abnormal P2X7 signaling plays a role in leukemia. We recently demonstrated that overexpression of P2X7 could not transform normal hematopoietic stem/progenitor cells into leukemia cells.[11] However, the role and mechanism of action of P2X7 in leukemia progression have not been elucidated.

Diverse endogenous and microenvironmental abnormalities contribute to the pathogenesis and progression of highly heterogeneous leukemias.[12-15] Chromosomal translocations involving the mixed lineage leukemia (MLL) gene are detected in nearly 80% of infants and 10% of adults with acute leukemia, and these patients often have unfavorable clinical outcomes.[16] Although more than 70 partners have

been identified in *MLL*-rearranged leukemia, the most common translocation partners are *AF4*, *AF9*, *ENL*, *AF10* and *ELL*.[17] Among these, *MLL-AF9* accounts for approximately 30% of cases of *MLL*-rearranged acute myeloid leukemia (AML).[18] Given the broad range of partners, different mechanisms by which MLL fusion proteins cause leukemia have been suggested, with abnormalities in the epigenetic regulatory network being considered the most important events.[19] Nevertheless, constitutive activation of homeobox (HOX) genes by fusion proteins is suggested as the central mechanism causing aberrant self-renewal in many *MLL*-rearranged cases of leukemia.[20] HOX proteins form cooperative DNA binding complexes with other atypical homeodomain proteins, such as PBX and MEIS, which belong to the three-amino-acid loop extension (TALE) family.[21] HOXA7, HOXA9 and cofactor MEIS1 are suggested to be key mediators in the transformation caused by *MLL* rearrangements.[22] Notably, increased expression of HOX proteins and their cofactors has also been detected in other leukemia subtypes.[23] Overexpression of the *Hox* gene with *Meis* induces leukemogenesis.[24] Furthermore, coexpression of *PBX3* and *MEIS1* is sufficient to transform normal hematopoietic stem/progenitor cells and induce AML in mice.[25] Hence, dysfunction of these factors plays important roles in different subtypes of leukemia.

Although P2X7 was suggested to have adverse effects in leukemia, the molecular mechanism has not been elucidated. In this study, we analyzed the correlation between P2X7 expression and clinical outcome and explored the mechanism of action of P2X7 in leukemia progression using mouse AML, nude mouse xenograft and patient-derived xenograft models. High levels of expression of P2X7 were correlated with worse survival in AML. Furthermore, P2X7 accelerated AML progression by promoting proliferation and increasing leukemia stem cells (LSC). Moreover, Pbx3 mediated the effects of P2X7.

Methods

Patients' samples

Bone marrow samples were collected from 20 newly diagnosed AML patients (*Online Supplementary Table S1*) and 12 normal donors at the Blood Diseases Hospital, Chinese Academy of Medical Sciences and Peking Union Medical College with informed consent (ethical review approval number KT2018045-EC-2).

Mouse acute myeloid leukemia models

All animal experiments were approved by the Animal Care and Use Committee at the institution.

To establish a mouse AML model overexpressing P2X7, GFP^+ cells were sorted from mice with *MLL-AF9*-induced AML[15] and infected with blank or pMSCV-P2X7 retrovirus. GFP^+BFP^+ cells were sorted and transplanted into C57BL/6J mice by intravenous tail injection. These cells were named MA9 and MA9-P2X7 cells, and the corresponding AML mice were named MA9 and MA9-P2X7 mice, respectively.

To establish mouse Pbx3 knockdown (KD) AML models, MA9-P2X7 cells were infected with pLV-SC or pLV-mPbx3sh1 lentiviruses. $GFP^+BFP^+RFP^+$ cells were sorted and transplanted into C57BL/6J mice. These cells were named MA9-P2X7-SC and MA9-P2X7-mPbx3sh1, and the corresponding AML mice were named MA9-P2X7-SC and MA9-P2X7-mPbx3sh1 mice, respectively.

Characterization of *MLL-AF9*-induced acute myeloid leukemia mouse models overexpressing P2X7

In most experiments, 3×10^5 MA9 or MA9-P2X7 cells were transplanted. In limiting-dilution transplantation experiments, 1×10^2, 1×10^3 and 1×10^4 MA9 or MA9-P2X7 cells were transplanted (n≥7). In Pbx3 KD experiments, 1×10^5 $GFP^+BFP^+RFP^+$ leukemia cells were transplanted (n=12). Leukemia cells in the peripheral blood, bone marrow and spleen were monitored, and the survival of mice was recorded. The cell cycle stage and apoptosis rate of freshly sorted leukemia cells were studied. In homing experiments, 9×10^6 leukemia cells were transplanted, and mice were sacrificed 16 h later (n=4). Total bone marrow and spleen cells were counted, and the proportion of leukemia cells was determined by flow cytometry.

Microarray studies

MA9, MA9 c-Kit^+, MA9 c-Kit^- and MA9-P2X7 cells were sorted by FACS. The microarrays were carried out by Oebiotech using Agilent Mouse Gene Expression (Format: 8*60K, Design ID: 028005). Feature Extraction software (version 10.7.1.1, Agilent Technologies) was used to obtain raw data, and Genespring software (version 12.5; Agilent Technologies) was used for the basic analysis. The raw data were normalized with a quantile algorithm. Fold-change ≥2.0 was used as the cutoff for screening for differentially expressed genes (DEG). The K-Mean cluster was analyzed by MeV 4.8.1, and the Venn diagram was analyzed online (*http://bioinfogp.cnb.csic.es/tools/venny/*). Gene set enrichment analysis was used to determine the biological functions or pathways primarily affected by the DEG. The datasets are available in the NCBI Gene Expression Omnibus (GEO) database (GSE92969).

Statistical analysis

The results are represented as means ± standard error of mean. GraphPad Prism 6.0 (San Diego, CA, USA) and SPSS 16.0 (SPSS, Chicago, IL, USA) were used. An unpaired Student *t* test was used for comparisons between two groups, whereas one-way analysis of variance was used for comparisons among multiple groups. Survival curves were produced using Kaplan-Meier estimates. The results for the limiting-dilution transplantation assays were compared using extreme limiting dilution analysis (ELDA). $P<0.05$ was considered statistically significant.

Additional experimental procedures are described in the *Online Supplementary Appendix*.

Results

High levels of P2X7 expression correlate with worse prognosis in patients with acute myeloid leukemia

In this study we used several public free databases and datasets to analyze the expression of P2X7 and the correlation between P2X7 and other genes. The detailed characteristics of patients (in some cases including the type of treatment received) can be accessed from the websites summarized in *Online Supplementary Table S2*. To determine the overall expression pattern of P2X7 in hematopoietic malignancies, a large-cohort leukemia microarray dataset (GSE13204, n=1,962) was analyzed. P2X7 expression was significantly higher in AML and CLL but lower in acute B-cell lymphoblastic leukemia (B-ALL) and chronic myelogenous leukemia than in normal controls (Figure 1A). We detected its expression in 20 newly diagnosed AML patients (*Online Supplementary Table S1*) showing that its expression was higher in AML than in normal bone marrow (Figure 1B). To further assess its clinical sig-

nificance, AML cases from The Cancer Genome Atlas (TCGA) datasets were divided into P2X7^{high} and P2X7^{low} groups according to the median value of P2X7. The main characteristics of the patients and the types of treatment received in the two groups are shown in *Online Supplementary Table S3*. The overall survival and disease-free survival rates in the P2X7^{high} group were significantly lower than those in the P2X7^{low} group (Figure 1C and D). Analysis of different AML subtypes with cytogenetic abnormalities from GSE13204 demonstrated that the highest levels of P2X7 were observed in AML with t(11q23) (Figure 1E). Similar results were also obtained from the TCGA datasets (n=144) and GSE6891 dataset (n=355), although the level of P2X7 was not the highest

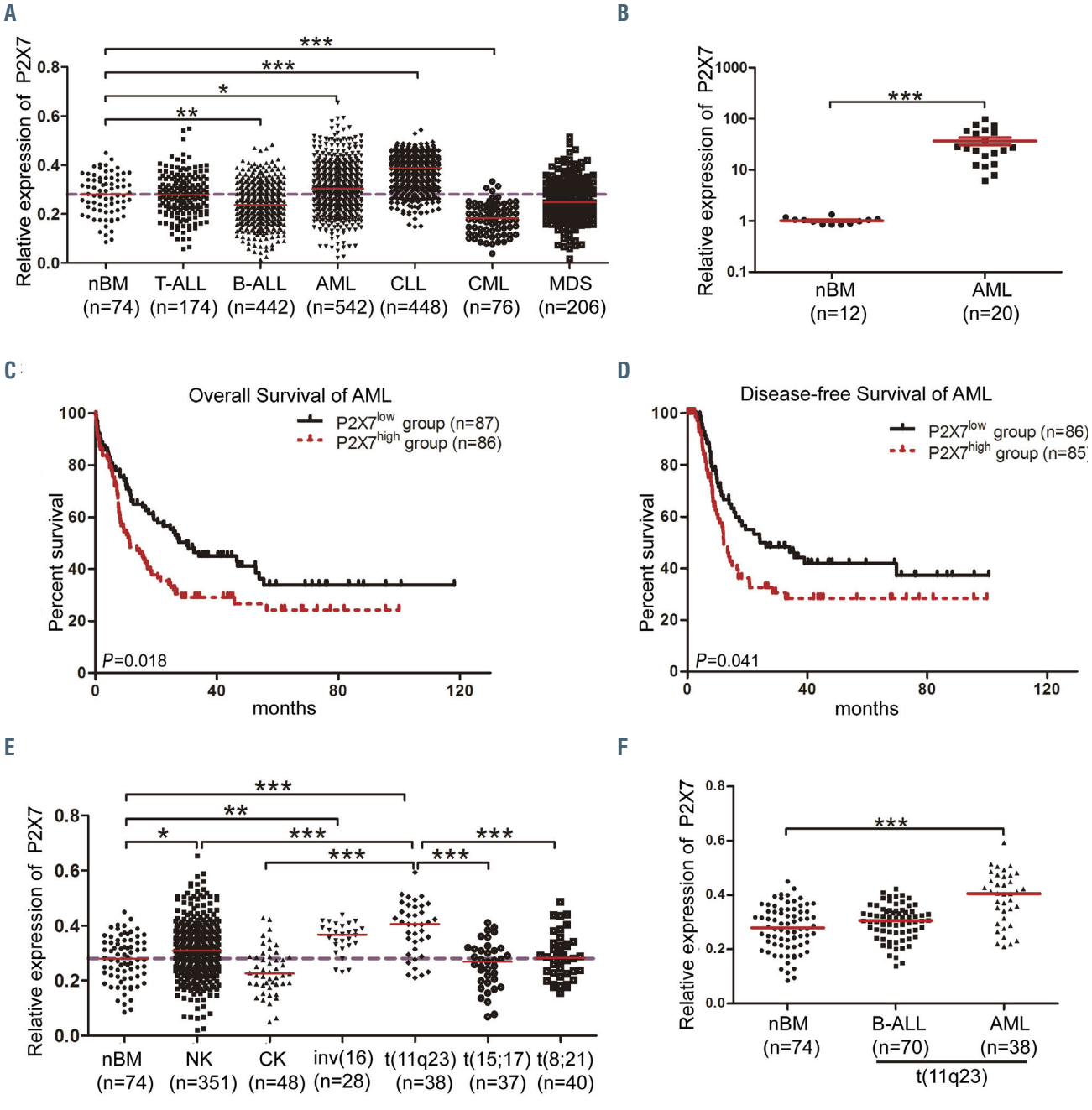

Figure 1. Expression of P2X7 in patients with hematopoietic malignancies. (A) The relative expression of P2X7 (from microarray experiments) in T-cell acute lymphoblastic leukemia (T-ALL), B-cell acute lymphoblastic leukemia (B-ALL), acute myeloid leukemia (AML), chronic lymphocytic leukemia (CLL), chronic myeloid leukemia (CML), myelodysplastic syndrome (MDS) and normal control bone marrow (nBM) was obtained from GSE13204. (B) The relative expression of P2X7 in newly diagnosed AML and nBM samples from the Blood Diseases Hospital was determined by assessed by quantitative real-time polymerase chain reaction. (C, D) Using data on AML patients from The Cancer Genome Atlas datasets (*https://tcga-data.nci.nih.gov/tcga*), the overall survival (C) and disease-free survival (D) of AML patients, divided into P2X7^{high} and P2X7^{low} groups according to the median value of P2X7, were compared by Kaplan-Meier analysis. (E) The relative expression of P2X7 in AML patients with normal karyotype (NK), complex karyotype (CK), inv(16), t(11q23), t(15;17), t(8;21) or nBM was obtained from GSE13204. (F) The relative expression of P2X7 in B-ALL with t(11q23), AML with t(11q23) and nBM was obtained from GSE13204. The dashed lines in (A) and (E) represent the median P2X7 expression in nBM (y=0.28). Bars represent the mean ± standard error of mean. **P*<0.05; ***P*<0.01; ****P*<0.001; unpaired Student t test and one-way analysis of variance.

(*Online Supplementary Figure S1A* and *B*). Furthermore, analysis of GSE13204 revealed that P2X7 expression was higher in t(11q23) AML than in t(11q23) B-cell acute lymphoblastic leukemia (Figure 1F). An overview from BloodSpot confirmed that P2X7 was highly expressed in *MLL*-rearranged AML (*Online Supplementary Figure S1C*). These findings suggest that high levels of P2X7 expression correlate with worse prognosis in AML and that P2X7 is highly expressed in *MLL*-rearranged AML.

Overexpression of P2X7 promotes the progression of *MLL*-rearranged acute myeloid leukemia

To study its significance in *MLL*-rearranged AML, P2X7 was overexpressed or suppressed in THP1 cells. Overexpression of P2X7 resulted in increased proliferation *in vitro* (Figure 2A and B). Suppression of P2X7 by either shRNA (*Online Supplementary Figure S2A*) or the inhibitor A740003 inhibited cell proliferation *in vitro* (Figure 2C-E). Furthermore, intratumoral administration of A740003 attenuated tumor formation in a nude mouse xenograft model (Figure 2F, *Online Supplementary Figure S2B*). These results suggest that high levels of P2X7 expression promote the progression of *MLL*-rearranged AML.

To further study the role of P2X7 in the progression of *MLL*-rearranged AML, the retrovirus pMSCV-P2X7-BFP was constructed. *MLL-AF9*-induced AML cells were infected with blank or recombinant retrovirus to construct AML mouse models (Figure 3A, *Online Supplementary Figure S3A*). All mice suffered from leukemia, and the AML cells from both models were GFP^+BFP^+ (*Online Supplementary Figure S3B* and *C*). The expression of P2X7 was verified by quantitative real-time polymerase chain reaction (qRT-PCR) analysis, western blot and immunofluorescence (Figure 3B). The function of P2X7 was further verified by measurement of the intracellular free Ca^{2+} concentration upon stimulation with BzATP, a specific P2X7 agonist, with or without KN62, a specific P2X7 inhibitor (Figure 3C). MA9 and MA9-P2X7 cells were both $CD3^-B220^-$. However, most MA9-P2X7 cells were $Gr1^+CD11b^+F4/80^+$, and approximately 2% of MA9-P2X7 cells were $CD115^+$, whereas the rates of positivity for Gr1, CD11b, F4/80 and CD115 in MA9 cells were 39.3%, 72.2%, 17% and 13.7%, respectively (*Online Supplementary Figure S3D*). Furthermore, MA9-P2X7 cells showed a more immature morphology, such as a larger cell size and less cytoplasm (*Online Supplementary Figure S3E*). More leukemia cells were detected in the bone marrow and spleen on day 10 in MA9-P2X7 mice (Figure 3E), and this was verified by hematoxylin & eosin staining of sections on day 12 (*Online Supplementary Figure S3F*). Importantly, the survival of MA9-P2X7 mice was shorter than that of MA9 mice (median 17.5 days *vs*. 25 days, respectively) (Figure 3D).

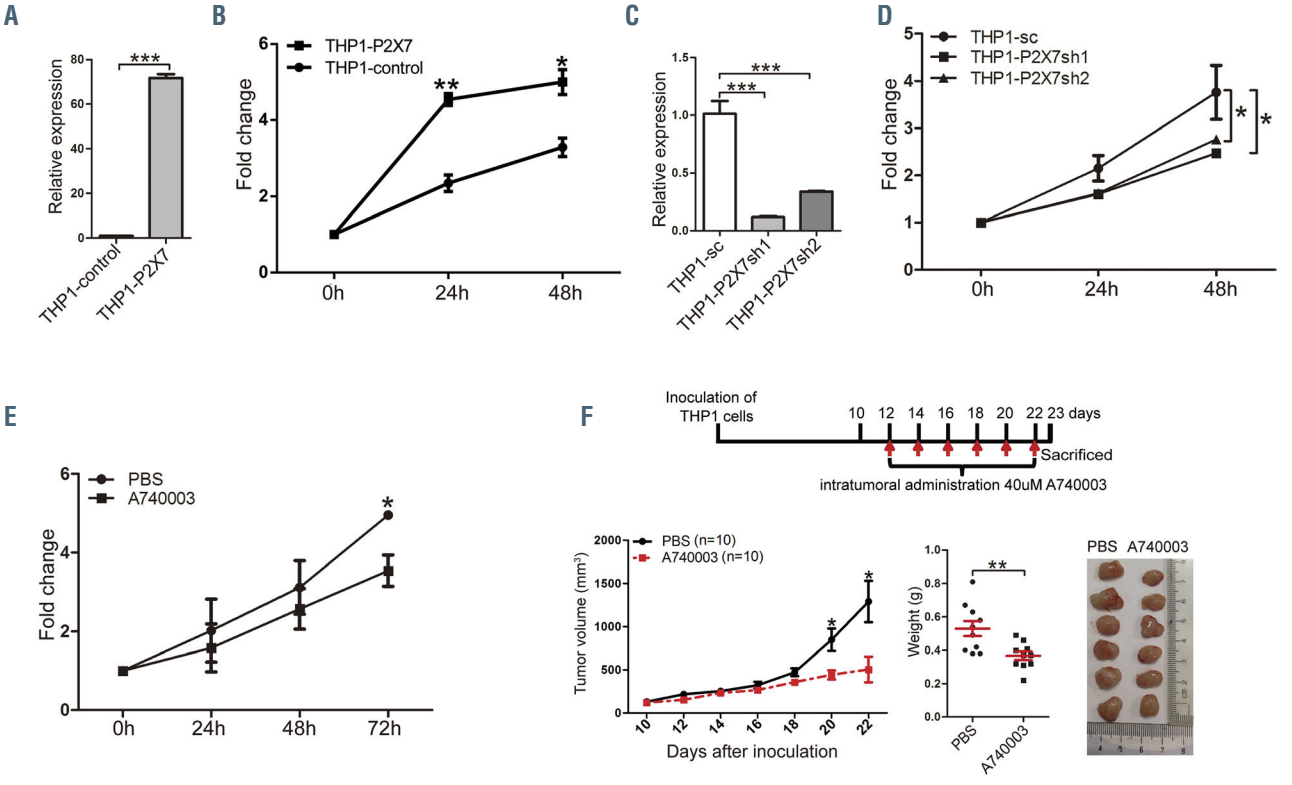

Figure 2. P2X7 promotes proliferation of THP1 cells. (A, B) THP1 cells were infected with blank retrovirus or retrovirus carrying P2X7. Forty-eight hours after infection, cells were sorted, the expression of P2X7 was determined by quantitative real-time polymerase chain reaction (qRT-PCR) (A), and cell proliferation was evaluated by an MTS assay (B). (C, D) THP1 cells were infected with blank lentivirus or lentivirus carrying shRNA against P2X7. Forty-eight hours after infection, the expression of P2X7 was determined by qRT-PCR (C), and cell proliferation was evaluated by an MTS assay (D). (E) Proliferation of THP1 cells with or without addition of A740003 *in vitro* was measured by an MTS assay. (F) The effects of P2X7 inhibition on the oncogenicity of THP1 cells were studied by comparing the consequences of intratumoral administration of A740003 or phosphate-buffered saline (PBS) in a nude mouse xenograft model. The experimental design is shown in the upper panel. Mice were sacrificed on day 23. Tumor volumes (*lower left panel*) and weights (*lower middle panel*) are plotted, and the typical size of tumors is shown (*lower right panel*). The results are from three independent experiments. Bars represent the mean ± standard error of mean. **P*<0.05; ***P*<0.01; ****P*<0.001; unpaired Student *t* test and one-way analysis of variance.

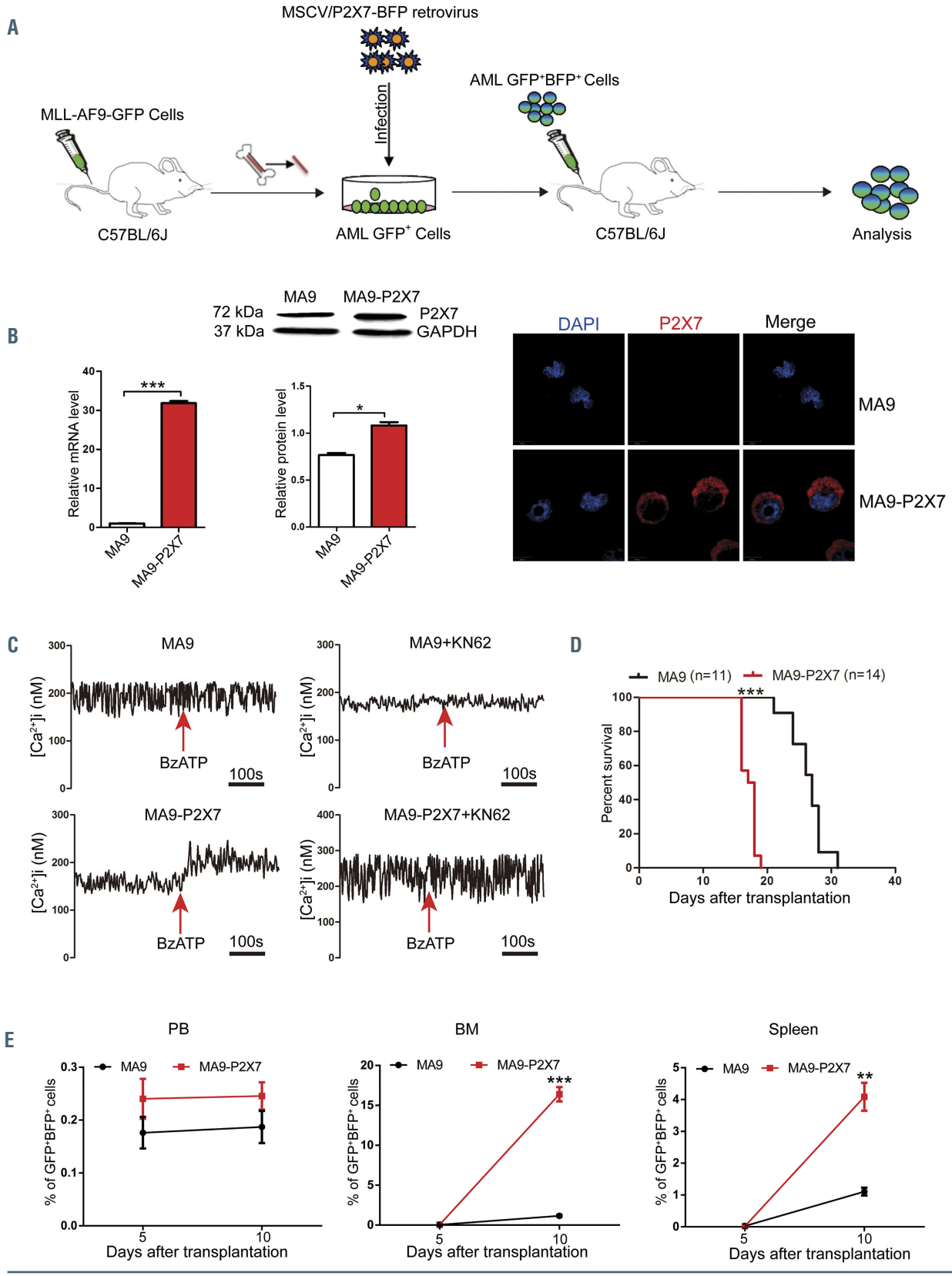

Figure 3. P2X7 accelerates leukemia progression in the mouse model of *MLL*-AF9-induced acute myeloid leukemia. (A) Experimental design for the establishment of a mouse model of *MLL-AF9*-induced acute myeloid leukemia (AML) overexpressing P2X7 (MA9-P2X7). (B) Mice were sacrificed, and GFP$^+$BFP$^+$ AML cells were sorted by flow cytometry. The expression of P2X7 was studied by quantitative real-time polymerase chain reaction (qRT-PCR) (*left*), western blot (*middle*) and confocal microscopy (*right*). The relative expression of P2X7 protein normalized to GAPDH is provided. P2X7 was stained with Dylight™649 (red), and nuclei were visualized with DAPI (blue). (C) The activity of P2X7 was verified by measurement of intracellular free Ca^{2+} concentration upon activation. Arrows indicate the addition of 100 mM BzATP. (D, E) GFP$^+$BFP$^+$ leukemia cells (3×10^5) were transplanted into recipient mice. Kaplan-Meier curves show the survival of leukemic mice (D), and the distribution of leukemia cells in peripheral blood (PB), bone marrow (BM) and spleen was determined every 5 days (n=3) (E). Bars represent the mean ± standard error of mean. *P<0.05; **P<0.01; ***P<0.001; unpaired Student t test.

Overexpression of P2X7 promotes proliferation of *MLL-AF9*-induced acute myeloid leukemia cells

The homing capability of leukemia cells was first studied to explore the mechanism. Unexpectedly, fewer AML cells (both as a proportion and in absolute numbers) were detected in the bone marrow and spleen of MA9-P2X7 mice than of MA9 mice, suggesting that P2X7 inhibited the homing of AML cells (Figure 4A). Next, cell proliferation and apoptosis were studied. An *in vivo* BrdU incorporation assay demonstrated that more S and G2/M phase but fewer G0/G1 phase cells were detected in MA9-P2X7 than in MA9 mice (Figure 4B). Ki67/Hoechst 33342 stain-

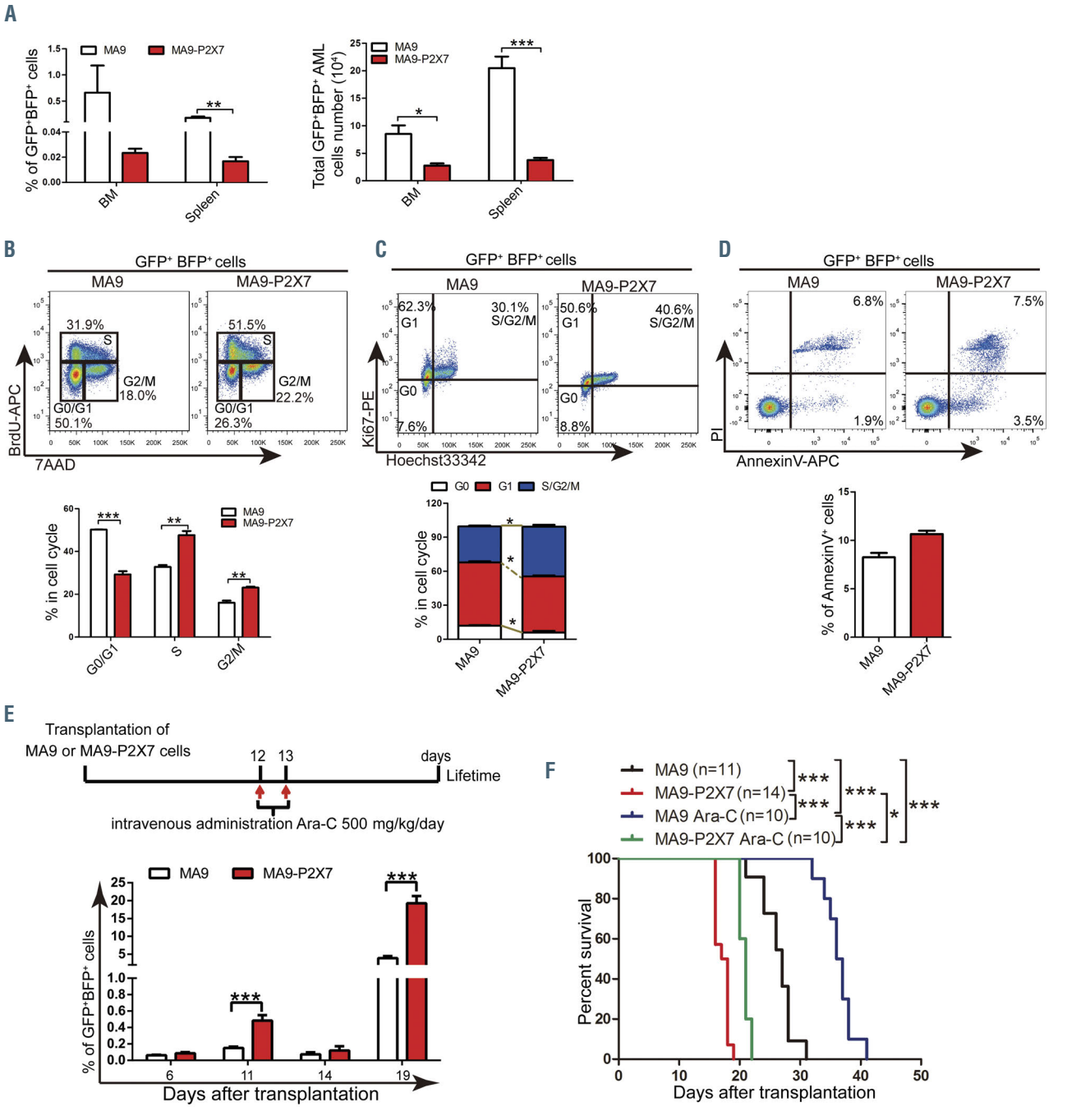

Figure 4. Characteristics of MA9-P2X7 cells. (A) The proportion (left panel) and total number (*right panel*) of GFP⁺BFP⁺ cells in the bone marrow (BM) and spleen were determined 16 h after the intravenous injection of 9×10^6 acute myeloid leukemia (AML) cells into recipient mice (n=4). (B) Leukemic mice were sacrificed 16 h after intraperitoneal injection of 200 μg of bromodeoxyuridine (BrdU). Leukemia cells were sorted and stained with BrdU-APC antibody and 7AAD. The gating strategy for G0/G1 (*bottom left*), S (top) and G2/M (*bottom right*) cells is shown (*top panel*). The percentages of these cells are plotted (n=3) (bottom panel). (C) Leukemia cells were sorted and stained with Ki67 and Hoechst 33342. The gating strategy for G0 (bottom left), G1 (*top left*), and S/G2/M (*top right*) is shown (*top panel*). The percentages of these cells are plotted (n=3) (bottom panel). (D) Leukemia cells were stained with annexin V and propidium iodide (PI). The gating strategy for early (*bottom right*) and late (*top right*) phase apoptotic cells is shown (*top panel*). The percentage of annexin V⁺ cells is plotted (n=3) (bottom panel). (E, F) Leukemic mice were treated twice with cytarabine (Ara-C) following the experimental design (E, *upper panel*). The percentages of peripheral blood leukemia cells before (days 6 and 11) and after (days 14 and 19) Ara-C treatments are plotted (E, bottom panel). Kaplan-Meier curves show the survival of the leukemic mice (F). Bars represent the mean ± standard error of mean. **P*<0.05; ***P*<0.01; ****P*<0.001; unpaired Student *t* test and one-way analysis of variance.

ing also showed similar results (Figure 4C). However, the rate of apoptosis of freshly isolated leukemia cells from the two groups was not significantly different (Figure 4D). We then assessed the response of the leukemic mice to cytarabine (Ara-C) treatment. After administration of a single dose of Ara-C to leukemic mice (with approximately 5% leukemia cells in peripheral blood), a more dramatic decrease in leukemia cells was observed in MA9-P2X7 mice than in MA9 mice. Following administration of multiple doses of Ara-C to leukemic mice (with approximately 10% leukemia cells), there were fewer leukemia cells in the peripheral blood in MA9-P2X7 mice than in MA9 mice at 48 h. Furthermore, more apoptotic cells were detected in the bone marrow of MA9-P2X7 mice than of MA9 mice (*Online Supplementary Figure S4A* and *B*). These results demonstrate that MA9-P2X7 cells are more sensitive to Ara-C treatment. To study whether MA9-P2X7 mice have survival advantages after Ara-C treatment, leukemic mice were given Ara-C twice. Although peripheral blood leukemia cell counts were decreased to almost identical levels in MA9 and MA9-P2X7 mice on day 14, the counts in MA9-P2X7 mice increased more rapidly, so that they were significantly higher on day 19 than in MA9 mice (Figure 4E), and MA9-P2X7 mice had a shorter survival than MA9 mice (Figure 4F). Moreover, the median survival was extended by 9.5 days (35.2%) in MA9 mice but by only 3.5 days (20.0%) in MA9-P2X7 mice. These results indicate that P2X7 promotes the proliferation of AML cells and imply that there are more LSC in MA9-P2X7.

Overexpression of P2X7 increases leukemia stem cell levels in *MLL-AF9*-induced acute myeloid leukemia

In vitro colony-forming ability was assessed to determine the self-renewal potential of leukemia cells. The MA9-P2X7 cells formed more colonies than did the MA9 cells (Figure 5A). The colonies were classified into three types:[26] type A colonies, which had a compact center; type B colonies, which had a dense center surrounded by a halo of migrating cells; and type C colonies, which consisted of many diffuse differentiating cells (*Online Supplementary Figure S5A*, left). MA9-P2X7 cells formed more type A, type B and type C colonies than did MA9 cells, especially type A colonies (*Online Supplementary Figure S5A*, right). High levels of LSC are associated with poor prognosis in AML. Limiting dilution transplantation experiments were used to analyze LSC frequency. In the groups transplanted with 10^3 cells, 100% of the MA9-P2X7 mice and 40% of the MA9 mice died from AML. Furthermore, 20% of the MA9-P2X7 mice and 0% of the MA9 mice suffered from AML in the groups given 10^2 cells (Figure 5B). The frequency of LSC was estimated to be 1/2088 in MA9 cells and 1/288 in MA9-P2X7 cells; this represents a 7.25-fold increase in functional LSC in MA9-P2X7 cells (Figure 5C). c-Kit, an important marker for LSC, was detected. Most MA9-P2X7 cells were c-Kit$^+$, whereas there were two populations of MA9 cells, more than half of which were c-Kit$^-$ (Figure 5D). Colonies of MA9 and MA9-P2X7 cells were collected and stained with c-Kit. The colonies showed similar results (*Online Supplementary Figure S5B*). Different populations were sorted and transplanted into recipient mice (*Online Supplementary Figure S5C*). MA9-P2X7 and MA9 c-Kit$^+$ cells gave rise to approximately 90% and 50% c-Kit$^+$ leukemia cells, respectively. Interestingly, MA9 c-Kit$^-$ cells also gave rise to more than 20% c-Kit$^+$ leukemia cells in serial transplantations (Figure 5E, *Online Supplementary Figure S5C*). Cell cycle analysis revealed that fewer G0/G1 but more S/G2/M phase cells were detected in c-Kit$^+$ MA9-P2X7 cells than in the other three populations (*Online Supplementary Figure S5D*). To further compare the malignant potential of these cells, equal numbers of MA9, MA9 c-Kit$^-$, MA9 c-Kit$^+$ and MA9-P2X7 cells were transplanted. Expectedly, MA9-P2X7 mice had the shortest survival time (Figure 5F). These results suggest that MA9-P2X7 cells are more malignant than MA9 and even MA9 c-Kit$^+$ cells.

Taken together, the results show that MA9-P2X7 cells have both greater proliferative potential and higher LSC frequency, which are characteristics that contribute to accelerated progression of leukemia.

Identification of key molecules mediating the pro-leukemic effects of P2X7

A gene expression microarray was used to screen key molecules mediating the effects of P2X7. MA9, MA9 c-Kit$^+$, MA9 c-Kit$^-$ and MA9-P2X7 cells were sorted and analyzed (*Online Supplementary Figure S6A*). The raw data were normalized to a quantile algorithm. The sum aggregate of DEG (n=3,329) and differentially expressed long non-coding RNA (n=1,940) were obtained. Hierarchical clustering analysis showed that MA9-P2X7 cells shared more similarities with MA9 c-Kit$^+$ than with MA9 or MA9 c-Kit$^-$ cells (*Online Supplementary Figure S6B*), which was in accordance with our previous observations. The DEG of MA9-P2X7 cells *versus* MA9, MA9 c-Kit$^+$ or MA9 c-Kit$^-$ cells are shown in a Venn diagram (Figure 6A). Furthermore, gene set enrichment analyses on different sets of DEG demonstrated that MA9-P2X7 cells had a more immature phenotype than that of MA9 cells and enhanced proliferative potential compared to that of MA9 c-Kit$^+$ or MA9 c-Kit$^-$ cells (Figure 6B). Analysis of the Gene Ontology (GO) and Kyoto Encyclopedia of Genes and Genomes (KEGG) databases for DEG between MA9-P2X7 and MA9 cells revealed that annotations related to membrane receptor signal transduction were highly enriched. Annotations related to differentiation and proliferation were also enriched (*Online Supplementary Figure S6C*). The 3,329 DEG were rearranged into 16 clusters based on their expression patterns in four samples. A cluster of genes (n=130) was highlighted since their expression was higher in MA9-P2X7 cells than in any other population. Fifty genes (*Online Supplementary Table S4*) were first selected since they satisfied the condition (fold-change ≥2.0) in all populations. After bloodspot analysis to examine positive correlations with P2X7 in leukemia patients, seven genes with high fold-change values were selected for further verification by qRT-PCR (primers are listed in *Online Supplementary Table S5*). Of these seven genes, three had homeodomains (Figure 6C). *Hoxa9*, *Meis1* and *Pbx2* were also included since they are important downstream regulators of *MLL*-rearranged leukemia. A high fold increase in *Pbx3* but not *Hoxa9*, *Meis1* or *Pbx2* was detected (Figure 6D). Furthermore, a significant positive correlation was detected between P2X7 and Pbx3 from the GSE10358, GSE19577 and GSE12417 AML datasets (Figure 6E), whereas such a correlation was found in the GSE10358 dataset only for HOXA9 (*Online Supplementary Figure S6D*) and MEIS1 (*Online Supplementary Figure S6E*), and no significant correlation was detected between P2X7 and PBX2 in the three

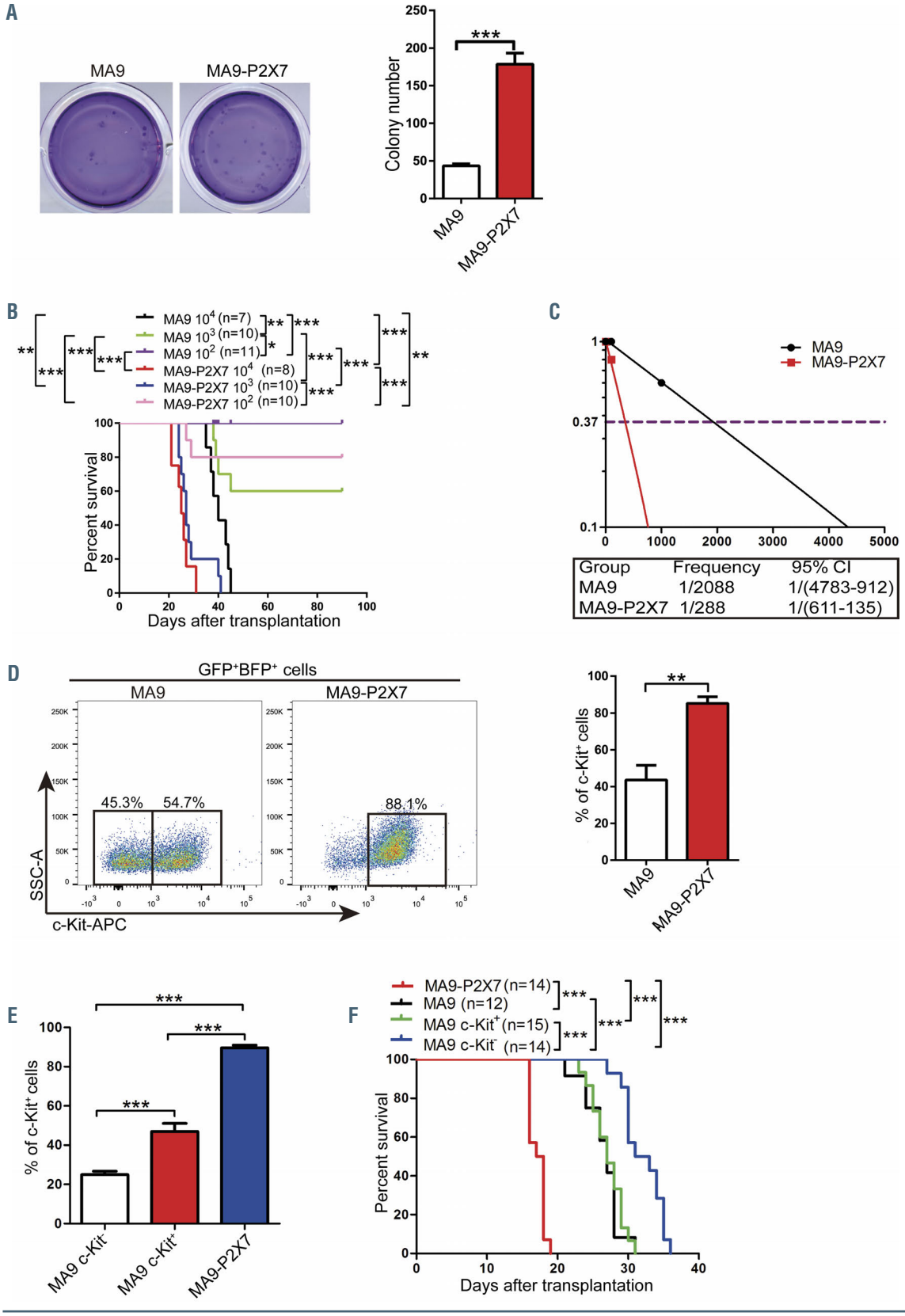

Figure 5. MA9-P2X7 cells have increased leukemia stem cells. (A) GFP$^+$BFP$^+$ leukemia cells were sorted and seeded onto 24-well plates (500 cells/well) for colony-forming assays. Typical Giemsa-stained dishes are shown (*left panel*), and colony numbers are plotted (*right panel*). (B) Different numbers of sorted GFP$^+$BFP$^+$ leukemia cells (1×10^4 and 1×10^3 for MA9 cells; 1×10^4, 1×10^3 and 1×10^2 for MA9-P2X7 cells) were transplanted into recipient mice, and the survival of mice was recorded. (C) The frequency of leukemia stem cells (LSC) was calculated using L-calc software. (D) Leukemia cells were stained with c-Kit. The gating strategy is shown (*left panel*), and the percentage of c-Kit$^+$ cells is plotted (*right panel*). (E) Sorted MA9 c-Kit$^-$, MA9 c-Kit$^+$ and MA9-P2X7 cells were transplanted into recipient mice. The percentage of c-Kit$^+$ leukemia cells was analyzed at the late stage of leukemia. (F) The same numbers of MA9, MA9 c-Kit$^-$, MA9 c-Kit$^+$ and MA9-P2X7 leukemia cells were transplanted into recipient mice, and survival was recorded. Bars represent the mean ± standard error of mean. *P<0.05; **P<0.01; ***P<0.001; unpaired Student t test and one-way analysis of variance. 95% CI: 95% confidence interval.

datasets (*Online Supplementary Figure S6F*). Moreover, upregulation of Pbx3 was observed in HL60 and Kasumi cells overexpressing P2X7 (*Online Supplementary Figure S6G*). Hence, Pbx3 was selected for further study.

Pbx3 mediates the pro-leukemic effects of P2X7 in *MLL*-rearranged acute myeloid leukemia

To study the role of Pbx3 in *MLL*-rearranged AML, MA9-P2X7 cells were infected with pLV-mPbx3-SC or pLV-mPbx3sh1 to construct control and Pbx3 KD AML models (*Online Supplementary Figure S7A*). The shRNA effectively decreased Pbx3 levels in MA9-P2X7-mPbx3sh1 cells (*Online Supplementary Figure S7B*). Fewer AML cells were detected in MA9-P2X7-mPbx3sh1 mice, especially on day 21, after transplantation of equal numbers of leukemia cells (Figure 7A). MA9-P2X7-mPbx3sh1 mice had smaller spleens and fewer leukemia cells than MA9-P2X7-SC mice on day 21 (Figure 7B). Importantly, MA9-P2X7-mPbx3sh1 mice survived longer than MA9-P2X7-SC mice (median survival: 34 days *vs.* 25 days, respectively) (Figure 7C). The *in vitro* colony-forming experiments demonstrated that MA9-P2X7-mPbx3sh1 cells formed fewer type A colonies than did MA9-P2X7-SC cells (Figure 7D), although there was not a significant difference between total colonies produced by the two types of cells (*Online Supplementary Figure S7C*). As type A colonies are relatively primitive, these results suggest that KD of Pbx3 decreases LSC levels.

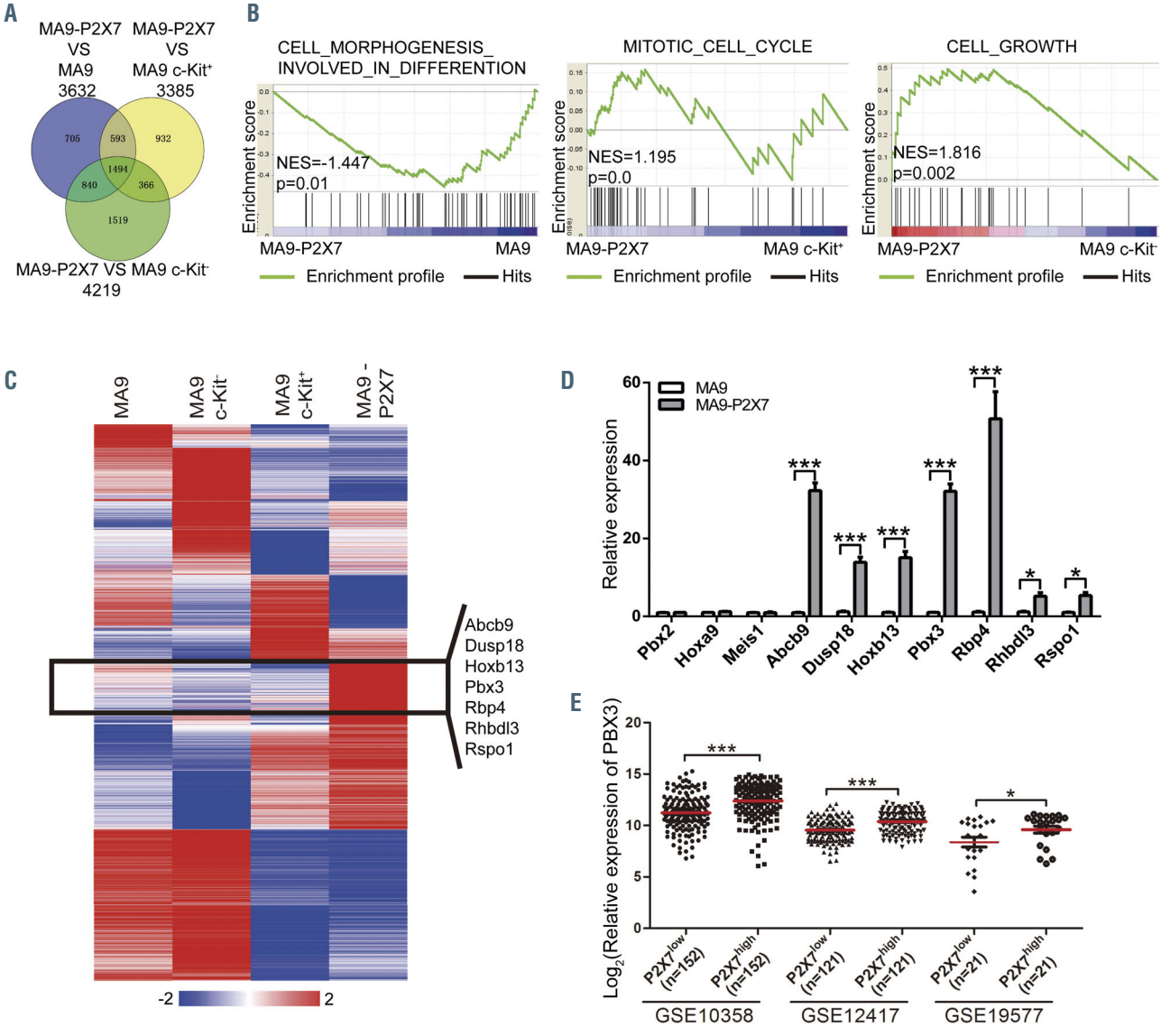

Figure 6. Identification of key molecules mediating the pro-leukemic effects of P2X7. MA9, MA9 c-Kit$^-$, MA9 c-Kit$^+$, and MA9-P2X7 cells were sorted, and microarray analysis was performed. (A, B) MA9-P2X7 was normalized to MA9, MA9 c-Kit$^+$ or MA9 c-Kit$^-$. The Venn diagram shows the overlap of differentially expressed genes (DEG) (A), which were subjected to gene set enrichment analysis (B). (C) K-mean clustering shows the 3,329 DEG (aggregate sum of DEG in four populations normalized to a quantile algorithm). The gene cluster and selected genes which were expressed at higher levels in MA9-P2X7 cells than in MA9, MA9 c-Kit$^-$ or MA9 c-Kit$^+$ cells are shown. (D) Selected genes were validated by quantitative real-time polymerase chain reaction. (E) The correlation between the relative expression of P2X7 and Pbx3 was studied from the GSE10358 (n=304), GSE12417 (n=242) and GSE19577 (n=42) datasets. For each dataset, AML cases were divided into P2X7^{low} and P2X7^{high} groups according to the median value of P2X7, and the relative expression of PBX3 is plotted. Bars represent mean ± standard error of mean. *P<0.05; ***P<0.001; one-way analysis of variance. NES: normalized enrichment score.

Endogenous Pbx3 in THP1 cells was suppressed by shRNA (*Online Supplementary Figure S7D*) with high efficiency (*Online Supplementary Figure S7E*). Inhibition of proliferation was observed *in vitro*, especially in THP1-hPbx3sh1 cells (Figure 7E). Furthermore, Pbx3 was also suppressed by hPbx3sh1 in leukemia cells from an AML patient with *MLL* translocation and high levels of P2X7 (*Online Supplementary Figure S7F-H*). Inhibition of proliferation was also detected (Figure 7F).

These results suggest that Pbx3 mediates the pro-leukemic effects of P2X7 in murine and human models of *MLL*-rearranged AML.

Discussion

Nucleotide-mediated signaling is becoming a research focus in various malignancies since it has been suggested to have important roles and therapeutic potential.[10] P2X7 is unique for its longest C-terminal intracellular domain of the P2X family of ATP-gated ion channels and for its formation of cytolytic pores permeable to large cations upon repeated or prolonged stimulation.[27] Mutations/polymorphisms of P2X7 have been identified in malignancies and abnormal expression has been detected in both malignant and microenvironmental cells.[9,28]

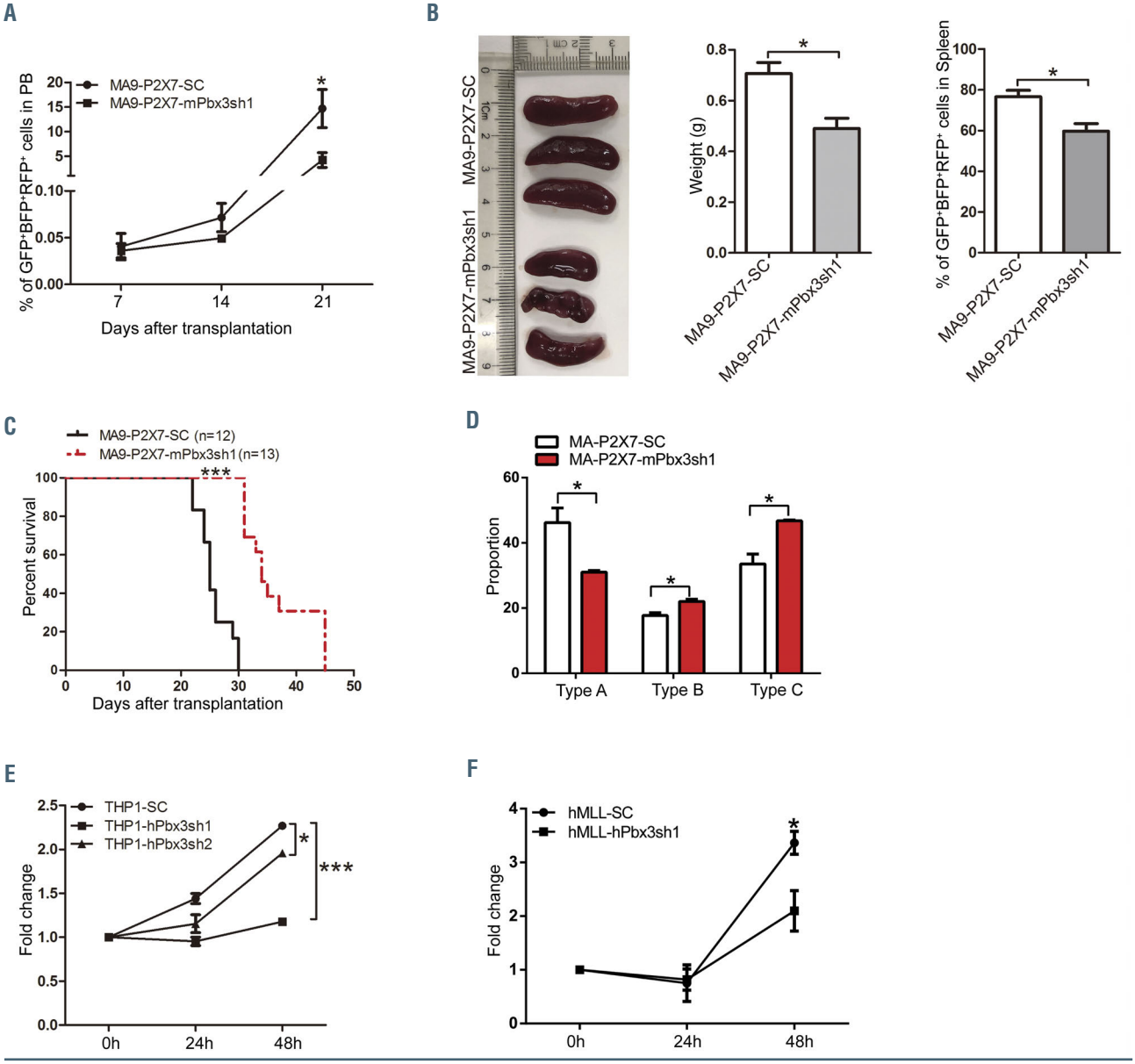

Figure 7. Pbx3 mediates the effects of P2X7 on proliferation and leukemia stem cell levels in acute myeloid leukemia cells with the *MLL-AF9* translocation. (A-D) Pbx3 was suppressed in MA9-P2X7 cells by shRNA against Pbx3. Equal numbers of MA9-P2X7-SC or MA9-P2X7-mPbx3sh1 cells were transplanted into recipient mice. The dynamic distribution of leukemia cells in peripheral blood (PB) is shown (A). The leukemic mice were sacrificed on day 21 and the size and weight of their spleens as well as the distribution of leukemia cells in the spleens were determined (B). Kaplan-Meier curves showing the survival of the leukemic mice (C). GFP$^+$BFP$^+$RFP$^+$ leukemia cells were sorted and seeded onto 24-well plates (500 cells/well) for colony-forming assays. The proportions of the different types of colony are shown (D). (E) THP1 cells were infected with blank lentiviruses or lentiviruses carrying shRNA against Pbx3. Forty-eight hours after infection, cells were sorted, and cell proliferation was studied by an MTS assay. (F) Pbx3 was knocked down in leukemia cells from an AML patient with an *MLL* translocation and a high level of P2X7 expression by shRNA. Forty-eight hours after infection, cells were sorted, and cell proliferation was studied by an MTS assay. The results are from three independent experiments. Bars represent mean ± standard error of mean. *P<0.05; ***P<0.001; unpaired Student t test and one-way analysis of variance.

However, the significance of P2X7 seems obscure since opposite effects have been observed.[29] Early studies focused on apoptosis caused by its cytolytic effects.[30] Exposure to high levels of ATP induces cell death in colon cancer due to disruption of the balance between cell growth and autophagy, which depends on the activation of the PI3K/AKT axis and AMPK-PRAS40-mTOR.[31] In contrast, P2X7 promotes cell growth in neuroblastoma, non-melanoma skin cancer, prostate cancer and thyroid papillary cancer by different mechanisms.[32] Typically, P2X7-dependent calcium influx results in the activation of downstream signaling pathways and the subsequent release of cytokines, inflammatory factors, microparticles, etc., which finally promote the proliferation and metastasis of tumor cells.[10]

Abnormal expression and function of P2X7 have been detected In various hematopoietic malignancies.[6-8] Overexpression of P2X7 failed to induce leukemic transformation,[11] but the role of P2X7 in leukemia progression remains largely unknown. Although an apoptosis-related mechanism was proposed in an early study,[30] leukemia is heterogeneous and it is thought that different mechanisms are involved in the initiation and progression of leukemia subtypes. We found that P2X7 was highly expressed in CLL and AML (Figure 1A) and that the levels of P2X7 in *MLL*-rearranged AML and CLL were equivalent (*Online Supplementary Figure S1C*). Adinolfi *et al.* reported that the expression of P2X7 was higher in evolutive B-cell CLL patients and suggested that high-level expression of P2X7 had a proliferative advantage and was associated with a poor prognosis in B-cell CLL.[8] However, the molecular mechanism in CLL has not been elucidated, partly because of the lack of appropriate cell lines and mouse models, although a mouse model based on B-cell-restricted expression of Sf3b1 mutation and Atm deletion has just been reported.[33] In contrast, there are suitable cell lines and mouse models to study the molecular mechanisms in AML, typically *MLL*-rearranged AML. Hence, we focused on AML. We found that overexpression of P2X7 accelerated the progression of *MLL*-rearranged AML by promoting proliferation and increasing LSC levels through the activation of the HOXA9/PBX3/MEIS1 axis by upregulation of Pbx3. Since more LSC and rapid proliferation are frequently related to worse clinical outcomes, our results suggest that P2X7 plays unfavorable roles in the progression of *MLL*-rearranged AML.

As a cofactor of Hoxa9, Pbx3 was previously thought to make a redundant contribution to cell transformation.[34] However, emerging evidence indicates that it has independent roles in leukemogenesis.[35] We demonstrated that the expression of Pbx3, but not of HOXA9 or MEIS1, is positively correlated with P2X7. Knockdown of Pbx3 in leukemia cells overexpressing P2X7 inhibited cell proliferation in different models, decreased LSC (forming type A colonies) and eventually prolonged the survival of AML mice. These effects of Pbx3 seem to be contradictory since LSC are considered a quiescent population.[36] However, leukemia cells comprise heterogeneous populations. Pbx3 not only plays vital roles in the maintenance of LSC[37] and tumor-initiating cells,[38] but also promotes the proliferation of non-LSC, which is also observed in solid tumors.[39] It is worth noting that there is still controversy about whether quiescence is necessary for LSC since there is evidence of a non-quiescent AML LSC population, which is required for the development of *MLL*-rearranged AML.[40] Hence, Pbx3 mediates the adverse effects of P2X7 in the progression of *MLL*-rearranged AML.

Although they have mainly been observed in models of *MLL*-rearranged AML, the effects and mechanism of P2X7 should also be present in other types of leukemia. P2X7^{high} AML had higher Pbx3 expression and worse prognosis than P2X7^{low} AML (Figures 6E and Figures 6F and 1C and D). Overexpression of P2X7 in leukemia cells without MLL rearrangements results in the upregulation of Pbx3. In fact, HOX proteins, which are also regulated by MEN1, CDX, etc.,[41] are widely involved in normal and malignant hematopoiesis.[42] Dysregulation of *HOX* gene expression is also found in other types of leukemia without *MLL* rearrangements, such as those with *PML-RARA*, *FLT*3-ITD and *NUP98*-related fusion genes.[43] Specifically, Pbx3 should play a role in the progression of other types of leukemia since upregulation of Pbx3 is detected not only in patients with *MLL* translocations[44] but also in those with *FLT*3-ITD and *NPM1* mutations as well as *NUP98*-related fusion genes.[43] This mechanism may also be involved in non-hematopoietic malignancies since Pbx3 is a key factor promoting metastasis, proliferation and poor prognosis in various solid tumors.[45] Pbx3 induces an infiltrative tumor cell phenotype in gastric cancer[46] and plays determinant roles in hepatocellular carcinoma tumor-initiating cells by regulating their self-renewal and tumorigenicity potential.[38] Hence, P2X7 may promote the progression of certain malignancies through the upregulation of Pbx3.

Although there is a positive correlation between P2X7 and Pbx3, the mechanism remains unclear. Abnormal activation of P2X7 is probably involved because high levels of ATP are detected in the microenvironment of various malignancies.[10] Ca^{2+} influx and K^+/Na^+ efflux, which may be involved in the P2X7-related upregulation of Pbx3, are early events upon P2X7 activation.[47] A rapid rise in intracellular Ca^{2+} concentration is an important event in the activation of hormone signals,[48] which regulates the expression of *HOX* genes.[49] Moreover, ion signaling is also required for post-translational modification of homeoproteins. For example, calcium binding to histone tails induces conformational changes essential for their functions.[50] Further work is required to elucidate the detailed interactions between P2X7 and Pbx3.

In summary, we provide compelling evidence that P2X7 accelerates the progression of *MLL*-rearranged AML by promoting proliferation and increasing LSC through the upregulation of Pbx3. This novel pathway links dysfunction in P2X7 signaling and poor clinical outcome in *MLL*-rearranged AML, and probably in other types of malignancies with high levels of P2X7 expression. Our study provides new insights into malignant progression caused by abnormal purinergic signaling.

Disclosures

No conflicts of interest to disclose.

Contributions

WF and XY designed the experiments, performed research and drafted the paper; they contributed equally to this work. RW, FY, HW, XL and RQ performed research and critically revised the paper. LW, YZ and XZ analyzed the data and critically revised the paper. GZ obtained funding, designed the experiments, acquired and analyzed the data and critically revised the paper. All authors are responsible for the accuracy and integrity of all aspects of the manuscript.

Funding

GZ was supported by the National Natural Science Foundation of China (grants 81770183, 81970155, 81170511 and 81570153), the Chinese Academy of Medical Sciences Innovation Fund for Medical Sciences (CIFMS) (grant 2016-I2M-2-006), and the Tianjin Natural Science Foundation (grant 17JCZDJC35000). LW was supported by CIFMS (grant 2017-I2M-1-015). WF and XY were supported by the Graduate Student Innovation Fund from Peking Union Medical College (grants 2014-0710-1021 and 2013-1001-021, respectively). GZ is a recipient of a New Century Excellent Talents in University award (NCET-08-0329).

References

1. Liu J. The dualistic origin of human tumors. Semin Cancer Biol. 2018;53:1-16.
2. Giuliani AL, Sarti AC, Di Virgilio F. Extracellular nucleotides and nucleosides as signalling molecules. Immunol Lett. 2019;205:16-24.
3. Di Virgilio F. Purines, purinergic receptors, and cancer. Cancer Res. 2012;72(21):5441-5447.
4. Amoroso F, Capece M, Rotondo A, et al. The P2X7 receptor is a key modulator of the PI3K/GSK3beta/VEGF signaling network: evidence in experimental neuroblastoma. Oncogene. 2015;34(41):5240-5251.
5. Amstrup J, Novak I. P2X7 receptor activates extracellular signal-regulated kinases ERK1 and ERK2 independently of Ca2+ influx. Biochem J. 2003;374(Pt 1):51-61.
6. Chong JH, Zheng GG, Zhu XF, et al. Abnormal expression of P2X family receptors in Chinese pediatric acute leukemias. Biochem Biophys Res Commun. 2010;391(1):498-504.
7. Zhang XJ, Zheng GG, Ma XT, et al. Expression of P2X7 in human hematopoietic cell lines and leukemia patients. Leuk Res. 2004;28(12):1313-1322.
8. Adinolfi E, Melchiorri L, Falzoni S, et al. P2X7 receptor expression in evolutive and indolent forms of chronic B lymphocytic leukemia. Blood. 2002;99(2):706-708.
9. Chong JH, Zheng GG, Ma YY, et al. The hyposensitive N187D P2X7 mutant promotes malignant progression in nude mice. J Biol Chem. 2010;285(46):36179-36187.
10. Di Virgilio F, Sarti AC, Falzoni S, et al. Extracellular ATP and P2 purinergic signalling in the tumour microenvironment. Nat Rev Cancer. 2018;18(10):601-618.
11. Feng W, Yang F, Wang R, et al. High level P2X7-mediated signaling impairs function of hematopoietic stem/progenitor cells. Stem Cell Rev. 2016;12(3):305-314.
12. Wang R, Feng W, Wang H, et al. Blocking migration of regulatory T cells to leukemic hematopoietic microenvironment delays disease progression in mouse leukemia model. Cancer Lett. 2020;469:151-161.
13. Wang R, Feng W, Yang F, et al. Heterogeneous effects of M-CSF isoforms on the progression of MLL-AF9 leukemia. Immunol Cell Biol. 2018;96(2):190-203.
14. Wang L, Feng W, Yang X, et al. Fbxw11 promotes the proliferation of lymphocytic leukemia cells through the concomitant activation of NF-kappaB and beta-catenin/TCF signaling pathways. Cell Death Dis. 2018;9(4):427.
15. Yang X, Feng W, Wang R, et al. Repolarizing heterogeneous leukemia-associated macrophages with more M1 characteristics eliminates their pro-leukemic effects. Oncoimmunology. 2017;7(4):e1412910.
16. Papaemmanuil E, Gerstung M, Bullinger L, et al. Genomic classification and prognosis in acute myeloid leukemia. N Engl J Med. 2016;374(23):2209-2221.
17. Meyer C, Burmeister T, Groger D, et al. The MLL recombinome of acute leukemias in 2017. Leukemia. 2018;32(2):273-284.
18. Stavropoulou V, Peters AHFM, Schwaller J. Aggressive leukemia driven by MLL-AF9. Mol Cell Oncol . 2018;5(3):e1241854.
19. Tsai CT, So CW. Epigenetic therapies by targeting aberrant histone methylome in AML: molecular mechanisms, current preclinical and clinical development. Oncogene. 2017;36(13):1753-1759.
20. Bach C, Buhl S, Mueller D, et al. Leukemogenic transformation by HOXA cluster genes. Blood. 2010;115(14):2910-2918.
21. Dard A, Reboulet J, Jia Y, et al. Human HOX proteins use diverse and context-dependent motifs to interact with TALE class cofactors. Cell Rep. 2018;22(11):3058-3071.
22. Collins CT, Hess JL. Role of HOXA9 in leukemia: dysregulation, cofactors and essential targets. Oncogene. 2016;35(9):1090-1098.
23. Schotte D, Lange-Turenhout EA, Stumpel DJ, et al. Expression of miR-196b is not exclusively MLL-driven but is especially linked to activation of HOXA genes in pediatric acute lymphoblastic leukemia. Haematologica. 2010;95(10):1675-1682.
24. Mamo A, Krosl J, Kroon E, et al. Molecular dissection of Meis1 reveals 2 domains required for leukemia induction and a key role for Hoxa gene activation. Blood. 2006;108(2):622-629.
25. Li Z, Chen P, Su R, et al. PBX3 and MEIS1 cooperate in hematopoietic cells to drive acute myeloid leukemias characterized by a core transcriptome of the MLL-rearranged disease. Cancer Res. 2016;76(3):619-629.
26. Lavau C, Szilvassy SJ, Slany R, et al. Immortalization and leukemic transformation of a myelomonocytic precursor by retrovirally transduced HRX-ENL. Embo J. 1997;16(14):4226-4237.
27. Di Virgilio F, Schmalzing G, Markwardt F. The elusive P2X7 macropore. Trends Cell Biol. 2018;28(5):392-404.
28. McCarthy AE, Yoshioka C, Mansoor SE. Full-length P2X7 structures reveal how palmitoylation prevents channel desensitization. Cell. 2019;179(3):659-670.
29. Kopp R, Krautloher A, Ramirez-Fernandez A, et al. P2X7 interactions and signaling - making head or tail of it. Front Mol Neurosci. 2019;12:183.
30. Locovei S, Scemes E, Qiu F, et al. Pannexin1 is part of the pore forming unit of the P2X(7) receptor death complex. FEBS Lett. 2007;581(3):483-488.
31. Bian S, Sun X, Bai A, et al. P2X7 integrates PI3K/AKT and AMPK-PRAS40-mTOR signaling pathways to mediate tumor cell death. Plos One. 2013;8(4):e60184.
32. Burnstock G, Knight GE. The potential of P2X7 receptors as a therapeutic target, including inflammation and tumour progression. Purinergic Signal. 2018;14(1):1-18.
33. Yin S, Gambe RG, Sun J, et al. A murine model of chronic lymphocytic leukemia based on B cell-restricted expression of Sf3b1 mutation and Atm deletion. Cancer Cell. 2019;35(2):283-296.
34. Laurent A, Bihan R, Omilli F, et al. PBX proteins: much more than Hox cofactors. Int J Dev Biol. 2008;52(1):9-20.
35. Li Z, Zhang Z, Li Y, et al. PBX3 is an important cofactor of HOXA9 in leukemogenesis. Blood. 2013;121(8):1422-1431.
36. Fujita S, Honma D, Adachi N, et al. Dual inhibition of EZH1/2 breaks the quiescence of leukemia stem cells in acute myeloid leukemia. Leukemia. 2018;32(4):855-864.
37. Guo H, Chu Y, Wang L, et al. PBX3 is essential for leukemia stem cell maintenance in MLL-rearranged leukemia. Int J Cancer. 2017;141(2):324-335.
38. Han H, Du Y, Zhao W, et al. PBX3 is targeted by multiple miRNAs and is essential for liver tumour-initiating cells. Nat Commun. 2015;6:8271.
39. Lamprecht S, Kaller M, Schmidt EM, et al. PBX3 is part of an EMT regulatory network and indicates poor outcome in colorectal cancer. Clin Cancer Res. 2018;24(8):1974-1986.
40. Zhang F, Liu X, Chen C, et al. CD244 maintains the proliferation ability of leukemia initiating cells through SHP-2/p27(kip1) signaling. Haematologica. 2017;102(4):707-718.
41. Alharbi RA, Pettengell R, Pandha HS, et al. The role of HOX genes in normal hematopoiesis and acute leukemia. Leukemia. 2013;27(5):1000-1008.
42. Bhatlekar S, Fields JZ, Boman BM. Role of HOX genes in stem cell differentiation and cancer. Stem Cells Int. 2018;2018:3569493.
43. Pan MM, Zhang QY, Wang YY, et al. Human NUP98-IQCG fusion protein induces acute myelomonocytic leukemia in mice by dysregulating the Hox/Pbx3 pathway. Leukemia. 2016;30(7):1590-1593.
44. Handschuh L. Not only mutations matter: molecular picture of acute myeloid leukemia emerging from transcriptome studies. J Oncol. 2019;2019:7239206.
45. Xu X, Bao Z, Liu Y, et al. PBX3/MEK/ERK1/2/LIN28/let-7b positive feedback loop enhances mesenchymal phenotype to promote glioblastoma migration and invasion. J Exp Clin Cancer Res. 2018;37(1):158.
46. Wang S, Li C, Wang W, et al. PBX3 promotes gastric cancer invasion and metastasis by inducing epithelial-mesenchymal transition. Oncol Lett. 2016;12(5):3485-3491.
47. Morrone FB, Gehring MP, Nicoletti NF. Calcium channels and associated receptors in malignant brain tumor therapy. Mol Pharmacol. 2016;90(3):403-409.
48. Foradori CD, Weiser MJ, Handa RJ. Non-genomic actions of androgens. Front Neuroendocrinol. 2008;29(2):169-181.
49. Daftary GS, Taylor HS. Endocrine regulation of HOX genes. Endocr Rev. 2006;27(4):331-355.
50. Holbert MA, Marmorstein R. Structure and activity of enzymes that remove histone modifications. Curr Opin Struct Biol. 2005;15(6):673-680.